Energy 54 (2013) 372–377

Contents lists available at SciVerse ScienceDirect

Energy

journal homepage: www.elsevier.com/locate/energy

Experiment on thermal uniformity and pressure drop of exhaust heat exchanger for automotive thermoelectric generator

Hongliang Lu [a,b], Ting Wu [a], Shengqiang Bai [a,*], Kangcong Xu [b], Yingjie Huang [b], Weimin Gao [c], Xianglin Yin [a], Lidong Chen [a]

[a] CAS Key Laboratory of Energy Conversion Materials, Shanghai Institute of Ceramics, Chinese Academy of Sciences, Shanghai 200050, China
[b] SAIC Motor Passenger Vehicle Co., Shanghai 201804, China
[c] BAIC Motor, Beijing 10028, China

ARTICLE INFO

Article history:
Received 19 October 2012
Received in revised form
23 January 2013
Accepted 19 February 2013
Available online 10 April 2013

Keywords:
Energy recovery
Thermoelectric generator
Automobile exhaust
Heat exchanger
Muffler

ABSTRACT

The power generation of exhaust TEG (thermoelectric generator) depends on heat energy and thermoelectric conversion efficiency. High efficiency heat exchanger is necessary to increase the amount of heat energy extracted from exhaust gas. On one hand, heat transfer is coupled with pressure drop for typical heat exchanger; on the other hand, the muffler unavoidably leads exhaust to large pressure drop for noise reduction. The present work tried to conceptually combine exhaust heat exchanger with muffler in the form of 1-inlet 2-outlet, 2-inlet 2-outlet and the baseline empty cavity. A test bench was developed to compare thermal uniformity and pressure drop characteristics over multiple vehicle operating conditions. 1-Inlet 2-outlet increased hydraulic disturbance and enhanced heat transfer, resulting in the more uniform flow distribution and higher surface temperature than the other. However, the averaged surface temperature was less than 100 °C, significantly limiting thermoelectric conversion efficiency. The pressure drops of 1-inlet 2-outlet, 2-inlet 2-outlet were 165%, 318% more than that of empty cavity when inlet temperature was 100 °C and mass flow rate was 131 kg/h, and were 319%, 523% more than that of empty cavity when inlet temperature 400 °C and mass flow rate 156 kg/h.

1. Introduction

For gasoline engine, about 40% of the primary gasoline energy is discharged as waste heat in exhaust gas [1]. The automotive exhaust is low in specific heat and small in time-averaged mass flow rate, so that an efficient heat exchanger is essential to extract heat energy from exhaust when thermoelectric conversation of conventional materials is 5%–7% for thermoelectric generator (TEG). Historically, several types of heat exchanger and different heat transfer enhancement measures such as the ribbing, grooving and protrusions have been investigated since the first automobile TEG was built in 1963. Serksnis [2] initially reported a stainless heat exchanger just like the exhaust pipe, no heat transfer enhancements were set in gas side. Birkholz et al. [3] designed a Hastelloy X rectangular heat exchanger with internal fins in exhaust side and an aluminum cold-side heat exchanger. Bass et al. [4] proposed a hexagonal cylinder and a center hollow displacement conic heat-diffuser for Cummins 14L NTC 350 diesel engine, discontinuous swirl fins were installed on surface of the center body to break laminar boundary layer and enhance gas turbulence. Thacher et al. [5] employed a rectangular, 1018 carbon steel compact heat exchanger with offset strip fins for a 5.3 L V8 gasoline engine. Crane et al. [6] improved thermal structure from a planar design to a cylindrical design with internal folded fins and stainless steel clad copper for BMW's 3 L inline six-cylinder engine. Su et al. [7] designed two different exhaust gas heat exchangers, and tested their acoustic characteristics, finally chose a "fishbone" finned internal structure with 12 mm interior thickness to increase thermal uniformity [8]. With the same requirements for exhaust heat exchanger in vehicle waste heat recovery by Rankine cycle, a shell and tube counter flow heat exchanger was used with exhaust gases in tubes and working fluids in shell [9].

For thermoelectric efficiency and generation capacity enhancement, heat exchanger's type, geometry, mounted location, contact area with thermoelectric modules, operating conditions and so on were optimized by numerical analyses and experiments. To obtain maximal net waste heat recovery performance, Crane et al. [10]

* Corresponding author. Tel.: +86 21 52412524; fax: +86 21 52413122.
E-mail address: bsq@mail.sic.ac.cn (S. Bai).

0360-5442/$ – see front matter © 2013 Elsevier Ltd. All rights reserved.
http://dx.doi.org/10.1016/j.energy.2013.02.067

integrated numerical cross flow heat exchanger model with TEG model, and optimized the hydraulic diameters of hot fluid, pitch of fins, pitch of tubes, height and width of thermoelectric legs in system level, the system with optimal design parameters could output a net power of 1000 W for a modestly sized heat exchanger. Chad et al. [11] compared 5 configurations by numerical model: single duct, single duct filled with porous metal foams, single duct with fins, multiple parallel counter flow ducts, and multiple serpentine-flow ducts, an unacceptable large pumping work requirement was found for the configurations using serpentine flow arrangement or porous media. Based on analytical method, the compromise programming was utilized to further improve the power density of TEG [12]. Astrain et al. [13] optimized the influence of heat exchangers' thermal resistances (in both the hot and cold side) and pressure drops by CFD [14] to maximize the electric power generated. Hsiao et al. [15] developed one dimensional thermal resistance model to predict TEG performance with two potential positions on an automobile: exhaust pipe and radiator. Wang [16] developed a three dimensional model to verify the significant effect of the variable properties and the heat losses to the ambient on thermoelectric conversion. The geometrical effect of TEG on heat transfer characteristics was investigated in a parallel microchannel heat sink [17]. Lagrandeur et al. [18] tested the pressure drop characteristics of TEG over a wide range of vehicle operating conditions, and the maximum static backpressure was about 60,000 Pa for the BMW X6. Katsunori et al. [19] proposed a reciprocating-flow super-adiabatic combustion in a catalytic and thermoelectric porous element, and announced a thermal efficiency of 4.7%, almost equal to the conversion efficiency of the thermoelectric element itself. Martins [20] adopted a variable conductance heat pipe as high efficiency means to supply the heat to a sufficiently low temperature while still maintain a high heat transfer rate, it could protect TEG against the extreme temperatures found in exhaust systems.

The amount of heat energy extracted from automotive exhaust is very important to promote system thermoelectric conversion capacity and efficiency. On one hand, the muffler necessarily leads exhaust to large pressure drop for noise reduction; on the other hand for a certain typical heat exchanger in general, the larger pressure drop, the more heat is transferred. The objective of present work is to conceptually combine the exhaust heat exchanger with the muffler in the form of 1-inlet 2-outlet, 2-inlet 2-outlet based on the referenced empty cavity. The prototype exhaust heat exchangers were designed and fabricated. The test bench was built to evaluate thermal uniformity and pressure drop characteristics over a wide range of operating conditions.

2. Experimental setup

2.1. Three typical structures of exhaust heat exchanger

Two exhaust heat exchangers with muffler-like internal structure were proposed as 1-inlet 2-outlet and 2-inlet 2-outlet based on the referenced structure: empty cavity. There was nothing in the empty cavity shown in Fig. 1a, but for 1-inlet 2-outlet the inlet pipe was inserted deeply into the cavity and the main outlet pipe was divided into 2 branch outlets shown in Fig. 1b, 2-inlet 2-outlet included two same pipes in the outlet and inlet shown in Fig. 1c. For the consistence of comparison, 3 structures were in the same shell with 670 mm × 360 mm × 81 mm, all the inlet and outlet of the structures were 51 mm in diameter.

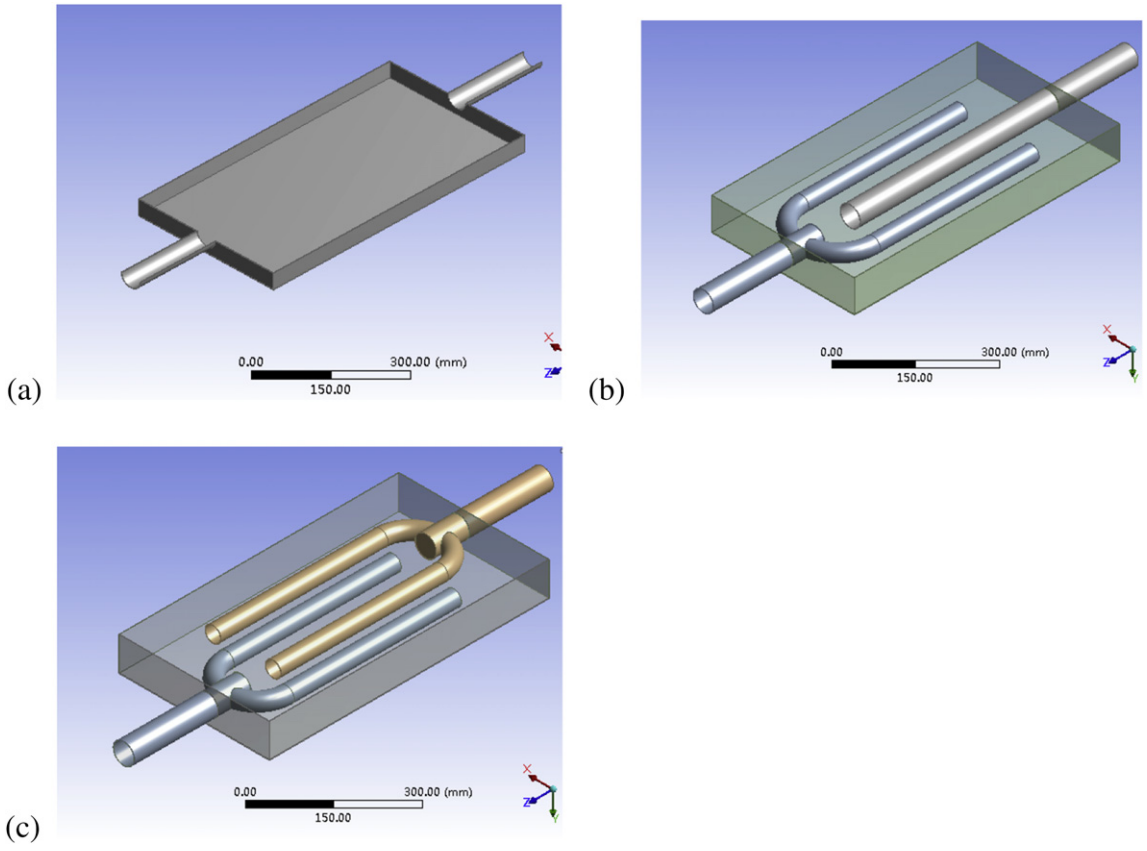

Fig. 1. Three internal structures: (a) Empty cavity, (b) 1-inlet 2-outlet, (c) 2-inlet 2-outlet.

Fig. 2. Test bench.

2.2. Test instrument and bench

To verify the effect of internal structures, a test system was developed given in Fig. 2 and Table 1. It had three parts: heat source as automobile exhaust, transducers and data acquisition system. HBO Industrial heat fan was employed to provide hot air simulating automobile exhaust with temperature up to 400 °C. Several transducers were used: pressure transmitters, differential pressure transmitters, K-type thermocouples and infrared camera to record the temperature distribution of exhaust heat exchanger. Keithley 2701 with 20-channel 7701 module was used to scan and save test real-time data.

Given the dirty and abrasive automobile exhaust, a stainless V-cone flow meter was adopted. The fluid volume flow was obtained by differential pressure of fluid flow across a standard V-cone structure after calibration, and then the mass flow equaled the volume flow multiplied by the density of fluid at V-cone's temperature and pressure. Another differential pressure transmitter was also chosen to test fluid's pressure drop through the exhaust heat exchanger. Due to high temperature of exhaust, the connecting pipe with a certain length was essential to cool down the tested fluid in the pipe between wall tapping and the pressure transducer, because the operation temperature limit of pressure meter body was −40 to 125 °C.

2.3. Typical operating conditions

The automobile exhaust was approximately 300–500 kPa in pressure and 500–700 °C in temperature when just discharged from the engine cylinder [21], and the heat source or heating temperature played an important role [22]. The HBO industrial heat fan instead of vehicle engine provided hot air with up to 400 °C in temperature and 360 kg/h in mass flow, OMRON E5CZ digital temperature controller was used to set air outlet temperature and EDS series electronic frequency converter was employed to regulate the fan speed: 108–216 kg/h in mass flow without air valve, this included the general exhaust range of light-duty vehicle under typical driving operations: 144 kg/h and 600 °C [23], 55 kg/h–187 kg/h and 426°C–562.8 °C for sports utility vehicle [24].

During the test, the external surface of exhaust heat exchangers was clean, smooth and exposed to the ambient with 22 °C. There was a steady but nonuniform temperature distribution on the exposed surface of heat exchanger during steady state operation. The infrared thermal image of the temperature field was obtained with the emissivity 0.82 selected for stainless steel according to InfraTec instruction manual; meanwhile the mass flow, pressure, pressure drop and temperature were recorded as one operating point.

3. Measurement

The different thermal performance and pressure drop stemmed from temperature field and velocity field of heat exchanger. In this section, the exhaust heat exchangers with three different internal structures were compared on the test bench in thermal uniformity and pressure drop.

3.1. Thermal uniformity analysis

The temperature distribution of the exhaust exchanger was crucial for the TEG in three aspects: firstly, it determined the available thermoelectric material by maximum continuous operating temperature; secondly, it seriously affected the energy conversion efficiency of heat to electricity; thirdly, it dominated the uniformity of thermal stress in device level and module level, a nonuniform thermal stress made the contact between TE module and heat exchanger rough, or even worse produced permanent damages to TEG modules. The following comparison was conduct for three heat exchangers when inlet temperature was 400 °C and fan frequency increased from 25 Hz to 50 Hz, which meant the same inlet temperature and pressure.

For empty cavity structure, the hot air flowed out of the inlet and expands freely in the cavity shown in Fig. 3, the impact area of external surface was in the downstream area of inlet and hotter than the rest, but it was relatively small, the minimum and maximum face temperature were 75 °C in the corners near the inlet, 91 °C in the central zone, respectively, and the temperature distribution was nonuniform as a whole. It was the hot deformation and low machining accuracy that resulted in the inclined outlet and the inclined flow. The temperature rose and kept a similar but hotter distribution when the inlet temperature was 400 °C and inlet mass flow increases from 117 kg/h to 216 kg/h gradually.

In regard of 1-inlet 2-outlet structure, the hot air flowed out of the long inlet in the cavity body, expanded and reflected by the opposite wall, and then moved relatively uniform to the two branch outlets shown in Fig. 4. The impact area of high temperature was

Table 1
Test instrument.

Instrument	Type	Uncertainty	Test range
V-cone flow meter	LGV23	Sensor: ±0.5%, System: ±1%, Repeatability: ±0.1%	Working fluid: −60 to +550 °C, 0–272 kg/h, ambient: −30 to +65 °C
K-type	WRCKKD	±0.75%	0–1050 °C
Differential pressure transmitters	Honeywell STD924	±0.65%, stability: ±0.01%/Y	0–2.5, 0–100 kPa
Pressure transmitters	BP-80	±0.5%	0–1600 kPa
Heat source	HBO Industrial heat fan	Temperature: ±2 °C, electronic frequency converter: 20–50 Hz	0–360 kg/h, 20–400 °C, 0–40 kP
Infrared camera	InfraTec VarioCAM hr-inspect	±1.5 K (0–100 °C), ±2% (<0 and >100 °C)	−40–1200 °C

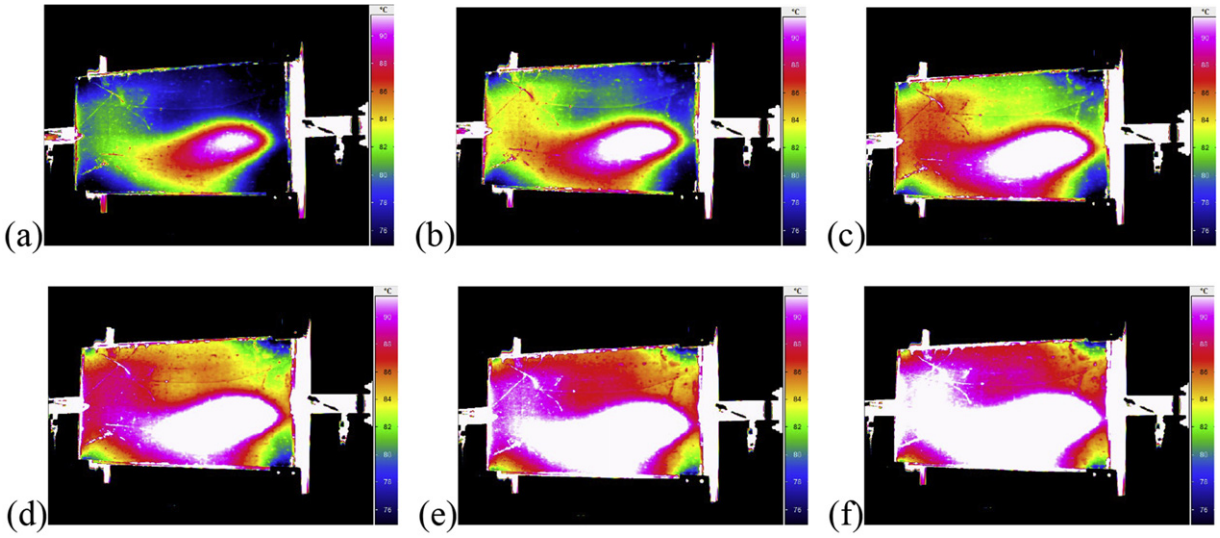

Fig. 3. Infrared thermal images of the empty cavity at 400 °C inlet temperature and mass flow: (a) 117 kg/h, (b) 138 kg/h, (c) 160 kg/h, (d) 180 kg/h, (e) 198 kg/h, (f) 216 kg/h.

around the wall against the internal inlet, the minimum and maximum face temperature were 70 °C in the corners near the outlets, 110 °C near the inlet, respectively, and its temperature distribution was more uniform than the empty cavity and 2-inlet 2-outlet. In the higher frequency fan rotated, the more air mass flowed, and the higher face temperature was. The temperature kept a similar but hotter distribution as the mass flow increased.

The 2-inlet 2-outlet structure was configured with two branch inlets and two branch outlets, this geometrical complexity increased hydraulic disturbance, resulting in the more pressure drop and lower face temperature given in Fig. 5 than the 1-inlet 2-outlet. The impact area near the wall facing the branch inlets was hotter than the rest, the minimum and maximum face temperature were 65 °C in the corners near the outlets, 97 °C near the outlets, respectively, and the temperature decreased gradually along the flow direction. The whole temperature field was also less uniform than 1-inlet 2-outlet because the lower right corner with low temperature was caused by asymmetrical branch outlets in 2-inlet 2-outlet. The increase in mass flow made less effect on the temperature field than the other structures.

The averaged surface temperature of exhaust heat exchangers was less than 100 °C, much below the inlet temperature 400 °C, this low temperature limited seriously thermoelectric conversion efficiency and capacity. From thermal resistance perspective, there were three causes for the phenomenon: firstly, the low mass flow led to small convection heat-transfer coefficient about 8.2 W/(m^2 °C) between exhaust gas and the heat exchanger wall; secondly, the external face area of the heat exchangers is as large as 0.62 m^2, its convective and radiation heat transfer are 387 W and 331 W, respectively when the free convection heat-transfer coefficient empirically assumed to be 8 W/(m^2 °C); thirdly, stainless steel had low thermal conductivity, 15.2 W/(m K), the higher the thermal resistance between the fluids was, the less heat flux was produced.

3.2. Performance comparison under typical operating conditions

The hot exhaust flowed into heat exchanger and transferred heat, which was bound to pressure drop for fluid. From a perspective of automobile engine, this pressure drop was equivalent to a rise in the ambient pressure and naturally a drop in output

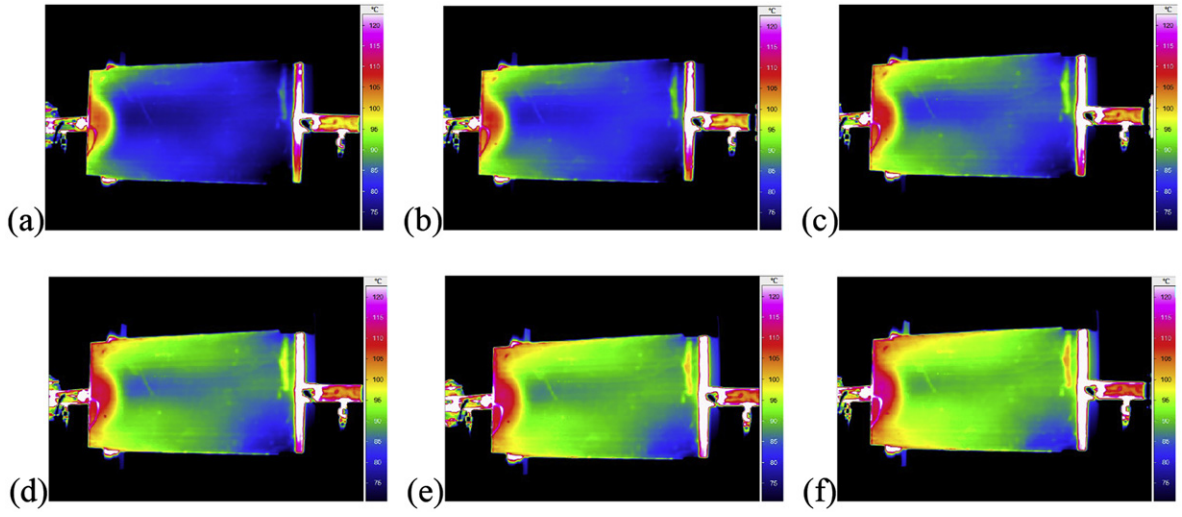

Fig. 4. Infrared thermal images of 1-inlet 2-outlet at 400 °C inlet temperature and mass flow: (a) 112 kg/h, (b) 135 kg/h, (c) 155 kg/h, (d) 174 kg/h, (e) 191 kg/h, (f) 202 kg/h.

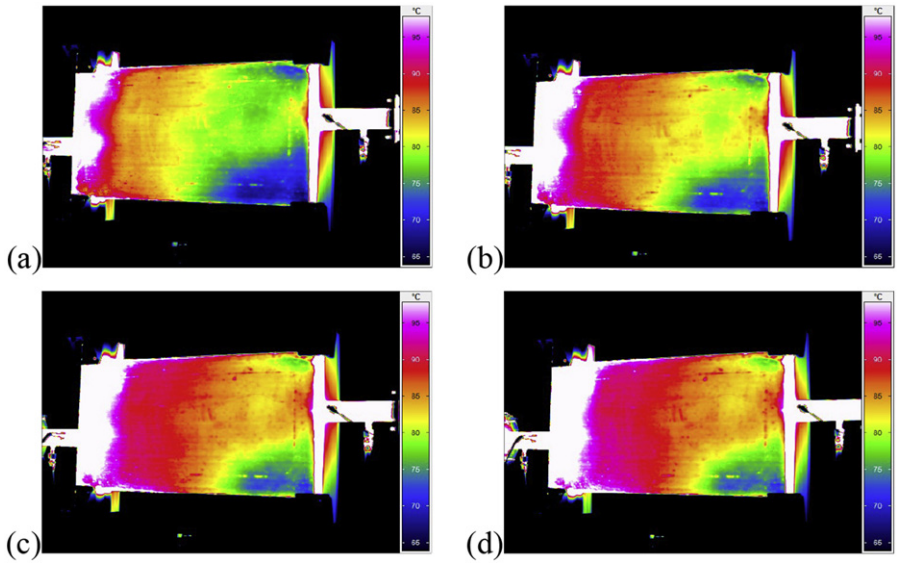

Fig. 5. Infrared thermal images of 2-inlet 2-outlet at 400 °C inlet temperature and mass flow: (a) 108 kg/h, (b) 129 kg/h, (c) 149 kg/h, (d) 156 kg/h.

power. In some cases, the maximum power output for example, the pressure drop may be high so seriously that the engine would stop working. It was necessary to test and evaluate pressure drop level of different structures under a wide range of operating conditions.

Corresponding to the different combinations of the inlet temperature: 100 °C, 200 °C, 300 °C, 400 °C and fan frequency: 25 Hz, 30 Hz, 35 Hz, 40 Hz, 45 Hz, 50 Hz, there were 24 operating conditions for one structure of exhaust heat exchanger. Due to the different hydraulic performance of internal structures, the three heat exchangers were different in practical mass flow from each other even when the inlet temperature and fan frequency were kept the same. As a result, the mass flow rather than fan frequency was chosen to compare the three heat exchangers in Fig. 6.

It was general for each structure: the more the mass flow rate was, the larger pressure drop was when the inlet temperature remained the same; the higher inlet temperature was, the larger pressure drop when the mass flow rate remained the same. But it also showed that the more complex the structure was, the larger pressure drop was, and the more scattered the pressure drop distribution was under multiple operating conditions. When inlet temperature was 100 °C and mass flow rate was about 131 kg/h, the empty cavity, 1-inlet 2-outlet, 2-inlet 2-outlet were 275 Pa, 730 Pa, 1150 Pa in pressure drop, respectively, that is the 1-inlet 2-outlet, 2-inlet 2-outlet were 165%, 318% more than empty cavity. And when inlet temperature rose to 400 °C and mass flow rate 19% to 156 kg/h, the three structures increased 25.8%, 98.6%, 117.6% to 346 Pa, 1450 Pa, 2503 Pa in pressure drop, respectively, that is the 1-inlet 2-outlet, 2-inlet 2-outlet were 319%, 523% more than empty cavity. Therefore, the pressure drop for structures increased in different growth with the mass flow rate: 2-inlet 2-outlet among

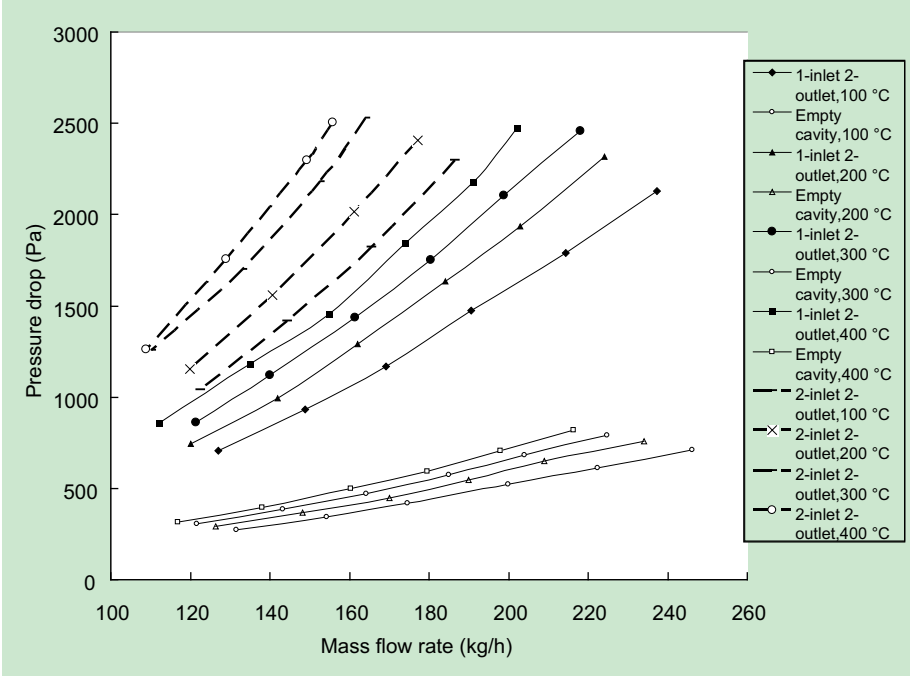

Fig. 6. Pressure drop of three structures under different conditions.

the three structures was always the largest in pressure drop and the most susceptible to temperature and mass flow rate, the opposite was the empty cavity.

Also shown in Fig. 6, the performance of exhaust heat exchanger such as the surface temperature and pressure drop was dependent on exchanger's type and geometry, operating condition, and the temperature field was coupled with flow field. The field synergy principle was proposed as an indication of the synergy degree between velocity and temperature field for the entire flow and heat transfer domain, the better the synergy was between the temperature field and velocity field, the better the heat transfer [25]. According to this theory, segmental baffles increased the field synergy number and brought performance improvement on the shell-and-tube heat exchanger [26]. 2-Inlet 2-outlet was more than the other in the field synergy number, but the cost was its pressure drop as large as 4–6 times of the empty cavity. The main content of the structure geometry modification of exhaust heat exchanger was enhanced heat transfer structures: to promote the variation of the velocity field and the uniformity of the temperature profile in the next stage.

4. Conclusion

A test bench was developed to test muffler-like exhaust heat exchangers with different structures. The symmetrical 1-inlet 2-outlet increased hydraulic disturbance and enhances heat transfer, resulting in the more uniform flow distribution and higher face temperature than the 2-inlet 2-outlet and empty cavity. The surface temperature of exhaust heat exchangers was less than 100 °C, seriously holding up thermoelectric conversion efficiency. The structure geometry modification of heat exchanger in the next stage was the promotion of the variation of the velocity field and the uniformity of the temperature profile.

1-inlet 2-outlet, 2-inlet 2-outlet were 455 Pa, 875 Pa, equally 165%, 318% more than empty cavity in pressure drop when inlet temperature was 100 °C and mass flow rate was about 131 kg/h. And they were 1004 Pa, 2157 Pa, equally 319%, 523% more when inlet temperature was 400 °C and mass flow rate was about 156 kg/h. 2-Inlet 2-outlet among the three structures was always the largest in pressure drop and the most dependent to temperature and mass flow rate.

Acknowledgments

The project was supported financially by International Science & Technology Cooperation Program of China, No. 2011DFB60150 and National Natural Science Foundation of China, Nos. 51102260 & 51004096. The authors are grateful to Science and Technology Development Fund Committee of Shanghai Automotive Industry.

References

[1] Yang Jihui, Stabler Francis R. Automotive applications of thermoelectric materials. Journal of Electronic Materials 2009;38:1245–51.
[2] Serksnis AW. Thermoelectric generator for automotive charging system. In: Proceedings of 11th Intersociety Conversion Engineering Conference. New York, USA; 1976, p. 1614–18.
[3] Birkholz U, Grob E, Stohre U, Voss K. Conversions of waste exhaust heat in automobiles using $FeSi_2$ thermoelements. In: Proceedings of the 7th International Conference on thermoelectric energy conversion. Arlington, USA; 1988, p. 124–8.
[4] Bass J, Elsner NB, Leavitt A. Performance of the 1 kW thermoelectric generator for diesel engines. In: Mathiprakisam B, editor. Proceedings of 13th International Conference on thermoelectrics, AIP Conference Proceedings. New York; 1995, p. 295–8.
[5] Thacher EF, Helenbrook BT, Karri MA, Richter CJ. Testing of an automobile exhaust thermoelectric generator in a light truck. Journal of Automobile Engineering 2007;221:95–107.
[6] Crane DT, Lagrandeur JW. Progress report on BSST-Led US Department of Energy automotive waste heat recovery program. Journal of Electronic Materials 2010;39:2142–8.
[7] Su CQ, Ye BQ, Guo X, Hui P. Acoustic optimization of automotive exhaust heat thermoelectric generator. Journal of Electronic Materials 2012;41:1686–92.
[8] Su CQ, Zhan WW, Shen S. Thermal optimization of the heat exchanger in the vehicular waste-heat thermoelectric generations. Journal of Electronic Materials 2012;41:1693–7.
[9] Domingues António, Santos Helder, Costa Mário. Analysis of vehicle exhaust waste heat recovery potential using a Rankine cycle. Energy 2013;49:71–85.
[10] Crane DT, Jackson GS. Optimization of cross flow heat exchangers for thermoelectric waste heat recovery. Energy Conversion and Management 2004;45:1565–82.
[11] Chad Baker, Vuppuluri Prem, Shi Li, Hall Matthew. Model of heat exchangers for waste heat recovery from diesel engine exhaust for thermoelectric power generation. Journal of Electronic Materials 2012;41:1290–7.
[12] Wang Chien-Chang, Hung Chen-I, Chen Wei-Hsin. Design of heat sink for improving the performance of thermoelectric generator using two-stage optimization. Energy 2012;39:236–45.
[13] Astrain D, Vián JG, Martínez A, Rodríguez A. Study of the influence of heat exchangers' thermal resistances on a thermoelectric generation system. Energy 2010;35:602–10.
[14] Martinez JG, Vian D, Astrain A, Rodriguez, Berrio I. Optimization of the heat exchangers of a thermoelectric generation system. Journal of Electronic Materials 2010;39:1463–8.
[15] Hsiao YY, Chang WC, Chen SL. A mathematic model of thermoelectric module with applications on waste heat recovery from automobile engine. Energy 2010;35:1447–54.
[16] Xiao-Dong Wang, Yu-Xian Huang, Chin-Hsiang Cheng, David Ta-Wei Line, Chung-Hao Kang. A three-dimensional numerical modeling of thermoelectric device with consideration of coupling of temperature field and electric potential field. Energy 2012;47:488–97.
[17] Rezania A, Rosendahl LA. Thermal effect of a thermoelectric generator on parallel microchannel heat sink. Energy 2012;37:220–7.
[18] Lagrandeur J, Crane D, Ayers Steve, Maranville C, Eder Andreas, Chiew Lee. High-efficiency thermoelectric waste energy recovery system for passenger vehicle applications. In FY 2009 annual progress report: advanced combustion engine R&D, solid state energy conversion 2009260–3.
[19] Katsunori Hanamura, Tomoyuki Kumano, Yuya Iida. Electric power generation by super-adiabatic combustion in thermoelectric porous element. Energy 2005;30:347–57.
[20] Martins J, Goncalves L, Antunes J, Brito F. Thermoelectric exhaust energy recovery with temperature control through heat pipes. SAE Technical Paper 2011. 2011-01-0315.
[21] Braess Hans-Hermann, Seiffer Ulrich. Handbook of automotive engineering [English version]. USA: SAE International; 2005.
[22] Chen Wei-Hsin, Liao Chen-Yeh, Hung Chen-I, Huang Wei-Lun. Experimental study on thermoelectric modules for power generation at various operating conditions. Energy 2012;45:874–81.
[23] Bell Lon E, Crane Douglas, LaGrandeur John, Ramesh Koripella C, Ayres Steven. Status of a thermoelectric segmented element. In: Waste heat power generator for vehicles, 2010 International Conference on Thermoelectrics; 2010.
[24] Karri MA, Thacher EF, Helenbrook BT. Exhaust energy conversion by thermoelectric generator: two case studies. Energy Conversion and Management 2011;52:1596–611.
[25] Guo ZY, Tao WQ, Shah RK. The field synergy (coordination) principle and its applications in enhancing single phase convective heat transfer. International Journal of Heat and Mass Transfer 2005;48(9):1797–807.
[26] Guo JF, Xu MT, Cheng L. The application of field synergy number in shell-and-tube heat exchanger optimization design. Applied Energy 2009;86(10):2079–87.